

- 11 (1975).  
 (35) J. M. Mallin, C. F. Schmdt, and H. E. Toma, *Inorg. Chem.*, **14**, 2924 (1975).  
 (36) P. Natarajan and J. F. Endicott, *J. Am. Chem. Soc.*, **94**, 5909 (1972).

- (37) J. G. Calvert and J. N. Pitts, "Photochemistry", Wiley, New York, N.Y., 1966, Chapter 3.  
 (38) H. Taube, "Electron Transfer Reactions of Complex Ions In Solution", Academic Press, New York, N.Y., 1970, Chapter 2.

## Matrix Photoionization Studies of Trifluoromethyl Halide Systems. Infrared Spectra of the $\text{CF}_3^+$ , $\text{CF}_2\text{X}^+$ , and $\text{CF}_3\text{X}^+$ Cations in Solid Argon

Frank T. Prochaska and Lester Andrews\*

Contribution from the Chemistry Department, University of Virginia, Charlottesville, Virginia 22901. Received September 12, 1977

**Abstract:** Photoionization of  $\text{CF}_3\text{X}$  ( $\text{X} = \text{Cl}, \text{Br}, \text{I}, \text{and H}$ ) samples by argon resonance radiation during condensation with excess argon at 15 K produced new infrared absorptions which were separated into distinct groups by mercury arc photolysis. Bands slightly reduced by photolysis are assigned to the daughter cations  $\text{CF}_3^+$  and  $\text{CF}_2\text{X}^+$  which were photoneutralized by transfer of electrons from halide ions. Absorptions markedly decreased by 340–1000-nm photolysis with the concomitant growth of  $\text{CF}_2\text{X}^+$  absorptions are assigned to parent cations  $\text{CF}_3\text{X}^+$ . Bands destroyed by 290–1000-nm photolysis are attributed to parent molecular anions. The cation  $\text{CF}_3^+$  exhibits a very high  $\nu_3$  fundamental which is consistent with extensive  $\pi(\text{p-p})$  bonding in this species.

### Introduction

The trichloromethyl cation has been produced by secondary hydrogen resonance photolysis of  $\text{CHCl}_3$ , proton radiolysis of  $\text{CCl}_4$ , and argon resonance photoionization of  $\text{CCl}_4$ , and trapped in solid argon for infrared spectroscopic study.<sup>1–3</sup> The relatively high antisymmetric carbon–chlorine stretching frequency,  $1037\text{ cm}^{-1}$ , suggests  $\pi$  bonding between the carbon and chlorines.

<sup>13</sup>C NMR studies of dimethylhalocarbenium ions have shown that fluorine interacts more effectively with the vacant p orbital on carbon than does chlorine.<sup>4,5</sup> The methyldifluorocarbenium ion has been prepared in superacid media,<sup>6</sup> but similar attempts to stabilize  $\text{CF}_3^+$  failed owing to reaction with  $\text{F}^-$  to form  $\text{CF}_4$ .<sup>7</sup> In order to learn more about the bonding and stability of these species, the simple trihalomethyl cations  $\text{CF}_2\text{X}^+$  ( $\text{X} = \text{F}, \text{Cl}, \text{Br}, \text{I}$ ) have been prepared for infrared spectroscopic study using the matrix isolation technique. A very recent matrix photoionization investigation of the  $\text{CFCl}_3$ ,  $\text{CF}_2\text{Cl}_2$ , and  $\text{CF}_3\text{Cl}$  compounds employed filtered high-pressure mercury arc photolysis of the samples to separate and identify the several molecular ions formed in these experiments, including the  $\text{CFCl}_2^+$  and  $\text{CF}_2\text{Cl}^+$  species.<sup>8</sup> The present study of  $\text{CF}_3\text{X}$  compounds provides infrared data on  $\text{CF}_3^+$ ,  $\text{CF}_2\text{X}^+$ , and the parent cations, and some insight into the bonding and photochemistry of these species.

### Experimental Section

The cryogenic equipment, vacuum systems, and matrix photoionization methods have been described previously.<sup>3,9–11</sup> The  $\text{CF}_3\text{X}$  compounds ( $\text{X} = \text{H}, \text{Cl} = \text{Br}, \text{and I}$ , Peninsular Chemresearch) were condensed at 77 K and evacuated to remove noncondensables. Carbon-13 enriched fluoroform was synthesized from the reaction of  $^{13}\text{CHCl}_3$  (90% <sup>13</sup>C, Merck Sharp and Dohme) with  $\text{FSO}_3\text{H}\cdot\text{SbF}_5$  (Magic Acid, Aldrich) which gave complete fluorination after 4 h. The fluoroform product was distilled from the reaction mixture at  $-127^\circ\text{C}$ . Samples of  $\text{Ar}/\text{CF}_3\text{X} = 200/1, 400/1, \text{and } 800/1$  were deposited on a CsI substrate at 14 K for 20 h with simultaneous irradiation from a windowless argon resonance lamp powered by a microwave discharge.<sup>11,12</sup> Since a comparable amount of argon from the discharge was condensed with the sample, the  $\text{Ar}/\text{CF}_3\text{X}$  ratio in

the matrix was double the sample value. The present experiments employed a 10-mm i.d. open-ended discharge tube. Samples of each reagent were also deposited for 20 h without photoionization to accurately measure the intensities and positions of all precursor absorptions. Infrared spectra were recorded during deposition to monitor product formation and after deposition on expanded wavenumber scales using a Beckman IR-12. Samples were photolyzed with filtered (water, transmits 220–1000 nm; water, Pyrex, transmits 290–1000 nm; and water, Pyrex, Corning 4303, transmits 340–1000 nm) BH-6 high-pressure mercury arc light and additional expanded scale spectra were scanned. The wavenumber accuracy is  $\pm 0.5\text{ cm}^{-1}$ . Band intensities were measured in absorbance units; comparisons of relative band intensities are accurate to better than 10%.

### Results

A series of matrix photoionization experiments was done with each trifluoromethyl halide and fluoroform.

**Trifluoromethyl Halides.** Figure 1 contrasts infrared spectra for samples of  $\text{CF}_3\text{Cl}$ ,  $\text{CF}_3\text{Br}$ , and  $\text{CF}_3\text{I}$  codeposited with simultaneous irradiation from the open argon discharge lamp. All of the spectra exhibited a sharp new feature at  $1666.5\text{ cm}^{-1}$  and water impurity lines at 1594, 1610, and  $1626\text{ cm}^{-1}$ .<sup>13</sup> Each precursor gave two new bands in the  $1520\text{--}1320\text{-cm}^{-1}$  region which depended on the heavier halogen. In the  $\text{CF}_3\text{Cl}$  experiments, the matrix split bands were dominated by sharp absorptions at 1515 and  $1514\text{ cm}^{-1}$ ; these features shifted to 1484 and  $1368\text{ cm}^{-1}$  in the  $\text{CF}_3\text{Br}$  run and to 1433 and  $1321\text{ cm}^{-1}$  in the  $\text{CF}_3\text{I}$  study. The sharp 1666- and  $1320\text{--}1520\text{-cm}^{-1}$  absorptions were slightly reduced by exposure to high-intensity mercury arc light using first 290–1000-nm and then 220–1000-nm filters.

The strongest new product band (labeled  $\text{P}^+$ ) in each experiment also showed a halogen shift from 1299 to 1293 or 1255 and to  $1229\text{ cm}^{-1}$  for the three precursors. The lowest illustrated spectral regions exhibited sharp product bands (also labeled  $\text{P}^+$ ) at 455, 469, and  $497\text{ cm}^{-1}$  for the  $\text{CF}_3\text{X}$  precursors. Of particular interest is the chlorine isotopic doublet at 733.5 and  $730.0\text{ cm}^{-1}$  in the  $\text{CF}_3\text{Cl}$  experiment. These  $\text{P}^+$  absorptions showed substantial reduction upon photolysis with 340–1000-nm BH-6 mercury arc light.

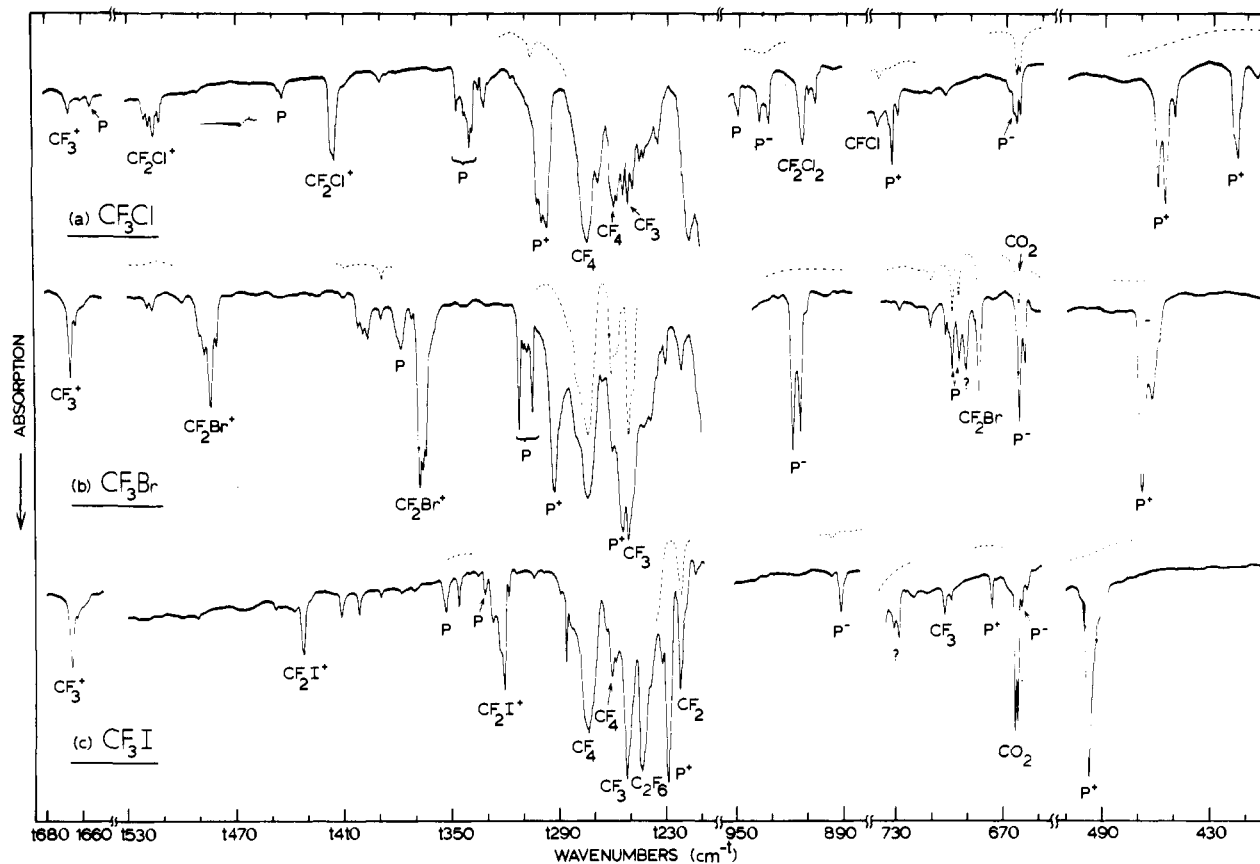


**Figure 1.** Infrared spectra following open discharge tube photoionization of trifluoromethyl halides during condensation with excess argon at 15 K for 20 h: (a) Ar/ $CF_3Cl$  = 300/1; (b) Ar/ $CF_3Br$  = 400/1; (c) Ar/ $CF_3I$  = 400/1. Since the samples were condensed with a comparable amount of argon, the reagent concentration in the matrix is half the sample value. The dashed inset scan with each trace shows changes caused by 290–1000-nm high-pressure mercury arc photolysis. Parent absorptions are labeled P.

Another group of absorptions (labeled  $P^-$ ) in the 940–890- and 660–666- $cm^{-1}$  spectral region also showed a halogen shift and exhibited different photolysis behavior; this group of absorptions was stable to 340-nm light but photolyzed with 290–1000-nm radiation. The dashed traces in Figure 1 illustrate changes in the spectrum for each precursor due to filtered 290–1000-nm BH-6 photolysis.

Tables I–III contrast the new product bands in the figure, and in addition give the band absorbances before and after several filtered mercury arc photolysis studies. This behavior proved to be a very important diagnostic technique for assigning infrared absorptions to different molecular species. In addition to absorptions due to new fluorohalocarbon species, absorptions<sup>14</sup> due to  $CF_2$ ,  $CF_3$ ,  $CF_4$ , and  $C_2F_6$  were observed, and these are listed in Table III.

Additional matrix reactions were conducted with sodium atoms and the trifluoromethyl halides for 20-h periods using techniques described previously<sup>9</sup> and a relatively low sodium concentration (Knudsen cell temperature 200 °C). In the  $CF_3Cl$  study, a weak NaCl band was observed at 335  $cm^{-1}$  in addition to a new feature at 945  $cm^{-1}$  (absorbance =  $A$  = 0.09), and  $CF_3$  at 1251  $cm^{-1}$  ( $A$  = 0.90). Photolysis with a medium-pressure mercury arc (AH-4, General Electric) for four 15-min periods produced a new doublet at 933 and 938  $cm^{-1}$  ( $A$  = 0.10) and a new band at 666  $cm^{-1}$  ( $A$  = 0.12), all three of which were observed in the argon photoionization study. Final photolysis with 290–1000-nm light from a BH-6 high-pressure arc changed the 938, 933  $cm^{-1}$  doublet to  $A$  = 0.12 and 0.06, respectively, increased the 666- $cm^{-1}$  band (0.14), and decreased the 945- $cm^{-1}$  feature ( $A$  = 0.05). The  $CF_3Br$  experiment with sodium atoms produced a weak NaBr band at 280  $cm^{-1}$ ,  $CF_3$  ( $A$  = 1.5 at 1251  $cm^{-1}$ ), and new

**Table I.** Product Absorptions ( $cm^{-1}$ ) and Intensities (Absorbance Units) Produced by Open Discharge Tube Photolysis of an Ar/ $CF_3Cl$  = 300/1 Sample for 20 h and the Effect of Filtered Mercury Arc Photolysis on the Absorption Intensities

Absorptions	Initial	30 min		Assignment
		340–1000 nm	120 min 220–1000 nm	
416	0.20	0.07	0.0	$CF_3Cl^+$
455	0.32	0.12	0.0	$CF_3Cl^+$
666	0.06	0.06	0.0	$CF_3Cl^-$
731	0.03	0.01	0.0	$CF_3^{37}Cl^+$
734	0.12	0.03	0.0	$CF_3^{35}Cl^+$
758	0.07	0.07	0.07	$CF_2^{37}Cl$
761	0.23	0.23	0.23	$CF_2^{35}Cl$
933	0.09	0.11	0.0	$CF_3Cl^-$
938	0.09	0.07	0.0	$CF_3Cl^-$
1148	0.75	0.75	0.75	$CF_2Cl$
1252	0.5	0.5	0.5	$CF_3$
1274	1.2	1.2	1.2	$CF_4$
1299	0.9	0.3	0.0	$CF_3Cl^+$
1415	0.23	0.24	0.15	$CF_2Cl^+$
1515	0.11	0.12	0.08	$CF_2Cl^+$
1666.5	0.04	0.04	0.03	$CF_3^+$

features at 668 ( $A$  = 0.15), 943 ( $A$  = 0.23), and 1130  $cm^{-1}$  ( $A$  = 0.25). Medium-pressure AH-4 photolysis for 35 min reduced these bands to  $A$  = 0.10, 0.15, and 0.10, respectively, and produced intense new bands at 918 ( $A$  = 0.33) and 662  $cm^{-1}$  ( $A$  = 0.26). A 30-min photolysis with 290–1000-nm BH-6 light reduced these new bands to  $A$  = 0.12 and 0.09, respectively, and further decreased the 668-, 943-, and 1130- $cm^{-1}$  features. A final 20-min exposure to 220–1000-nm BH-6 light destroyed these bands except for the one at 944

**Table II.** Product Absorptions ( $\text{cm}^{-1}$ ) and Intensities (Absorbance Units) in an Open Discharge Tube Experiment with an Ar/ $\text{CF}_3\text{Br} = 400/1$  Sample and Following Photolysis by Filtered Mercury Arc Light

Absorptions	Initial	35 min 340-1000 nm	35 min 290-1000 nm	125 min 220-1000 nm	Assignment
469	0.56	0.33	0.02	0.0	$\text{CF}_3\text{Br}^+$
662	0.20	0.20	0.0	0.0	$\text{CF}_3\text{Br}^-$
685	0.16	0.16	0.16	0.16	$\text{CF}_2\text{Br}$
692	0.11	0.08	0.0	0.0	?
914	0.32	0.34	0.0	0.0	$\text{CF}_3\text{Br}^-$
918	0.38	0.48	0.02	0.0	$\text{CF}_3\text{Br}^-$
959	0.11	0.09	0.0	0.0	?
1137	0.70	0.70	0.70	0.70	$\text{CF}_2\text{Br}$
1252	0.9	0.9	0.9	0.9	$\text{CF}_3$
1255	0.9	0.6	0.0	0.0	$\text{CF}_3\text{Br}^+$
1293	0.50	0.32	0.0	0.0	$\text{CF}_3\text{Br}^+$
1368	0.58	0.62	0.52	0.35	$\text{CF}_2\text{Br}^+$
1484	0.25	0.26	0.22	0.12	$\text{CF}_2\text{Br}^+$
1666.5	0.17	0.17	0.15	0.11	$\text{CF}_3^+$

**Table III.** Product Absorptions ( $\text{cm}^{-1}$ ) and Intensities (Absorbance Units) Produced by Open Discharge Photoionization of an Ar/ $\text{CF}_3\text{I} = 400/1$  Sample during Condensation at 15 K for 20 h<sup>a</sup>

Absorptions	Initial	35 min 340-1000 nm	120 min 220-1000 nm	Assignment
497	0.51	0.0	0.0	$\text{CF}_3\text{I}^+$
595	0.10	0.02	0.02	?
627	0.14	0.14	0.09	$\text{CF}_2\text{I}$
660	0.04	0.04	0.0	$\text{CF}_3\text{I}^-$
677	0.06	0.0	0.0	$\text{CF}_3\text{I}^+$
730	0.07	0.07	0.0	?
826	0.05	0.05	0.0	?
893	0.07	0.07	0.0	$\text{CF}_3\text{I}^-$
979	0.07	0.07	0.0	?
1103	0.72	0.42	0.32	$\text{CF}_2$
1111	0.05	0.06	0.13	$\text{C}_2\text{F}_6$
1126	0.70	0.68	0.51	$\text{CF}_2\text{I}$
1136	0.08	0.08	0.10	?
1205	0.85	0.85	1.2	$\text{C}_2\text{F}_x\text{I}_y$
1223	0.33	0.16	0.10	$\text{CF}_2$
1229	1.5	0.0	0.0	$\text{CF}_3\text{I}^+$
1244	0.6	0.7	1.0	$\text{C}_2\text{F}_6$
1252	0.6	0.7	1.0	$\text{CF}_3$
1274	0.5	0.7	1.1	$\text{CF}_4$
1305	0.01	0.03	0.07	?
1321	0.26	0.28	0.16	$\text{CF}_2\text{I}^+$
1402	0.04	0.04	0.03	?
1412	0.05	0.05	0.04	?
1433	0.10	0.11	0.07	$\text{CF}_2\text{I}^+$
1666.5	0.15	0.15	0.09	$\text{CF}_3^+$

<sup>a</sup> Mercury arc photolysis data are given for two filters.

$\text{cm}^{-1}$  ( $A = 0.06$ ). In the  $\text{CF}_3\text{I}$  reaction with sodium,  $\text{CF}_2$ ,  $\text{CF}_3$  ( $A = 1.5$  at  $1251 \text{ cm}^{-1}$ ), and  $\text{C}_2\text{F}_6$  were observed in addition to very strong new bands at  $655$  ( $A = 1.5$ ),  $849$ ,  $855$  ( $A = 1.5$ ),  $894$  ( $A = 0.09$ ),  $945$  ( $A = 0.07$ ), and  $1214 \text{ cm}^{-1}$  ( $A = 0.11$ ). Photolysis for 45 min with the AH-4 arc had no effect on the bands, while a 15-min exposure to the BH-6 arc using 290-1000-nm light reduced the major bands at  $655$  ( $A = 0.72$ ) and  $849$ ,  $855 \text{ cm}^{-1}$  ( $A = 0.40$ ), left the  $945\text{-cm}^{-1}$  feature unchanged, produced a sharp  $892\text{-cm}^{-1}$  band ( $A = 0.02$ ) on the side of the broad  $894\text{-cm}^{-1}$  absorption, increased the  $1214\text{-cm}^{-1}$  feature ( $A = 0.27$ ), and produced a new  $1300\text{-cm}^{-1}$  band ( $A = 0.13$ ). A final 220-1000-nm BH-6 photolysis destroyed the sharp  $892\text{-cm}^{-1}$  feature and substantially reduced the above product absorptions.

**Fluoroform.** Two photoionization experiments were done with fluoroform using Ar/ $\text{CHF}_3 = 200/1$  and  $800/1$  sample

concentrations. The  $1600\text{-cm}^{-1}$  region in this study is of particular interest, and it is illustrated in Figure 2. Trace (a) shows the spectrum of an Ar/ $\text{CHF}_3 = 200/1$  sample deposited without argon resonance photolysis; note the weak  $\text{CHF}_3$  combination ( $\nu_5 + \nu_6$ ) band<sup>15</sup> at  $1645 \text{ cm}^{-1}$  and the weak water absorptions at  $1626$ ,  $1610$ , and  $1594 \text{ cm}^{-1}$ . Trace (b) gives the spectrum recorded after photoionization of an Ar/ $\text{CHF}_3 = 800/1$  sample during deposition for 18 h; note the sharp ( $2.0 \text{ cm}^{-1}$  full width at half-maximum) intense ( $A = 0.15$ ) new band at  $1666.5 \text{ cm}^{-1}$ . In addition, the very strong  $1174\text{-}$  and  $1166\text{-cm}^{-1}$  and weaker  $1316\text{-cm}^{-1}$  bands<sup>16</sup> of the  $\text{CHF}_2$  radical were observed along with very strong absorptions due to the  $\text{CF}_2$ ,  $\text{CF}_3$  ( $A \sim 2.0$ ),  $\text{C}_2\text{F}_6$ , and  $\text{CF}_4$  species.<sup>14</sup> No absorptions were observed between  $1320$  and  $1580 \text{ cm}^{-1}$  except the very strong  $1377\text{-cm}^{-1}$   $\text{CHF}_3$  band. This sample was warmed to  $30\text{-}35 \text{ K}$  for 10 min until the  $1666\text{-cm}^{-1}$  band was reduced to  $A = 0.05$ ; the  $\text{CF}_2$  bands were eliminated, the  $\text{CF}_3$  absorption was reduced slightly, and the  $\text{CF}_4$  bands were increased slightly. Photoionization of an Ar/ $\text{CHF}_3 = 200/1$  sample produced more intense product absorptions; the new band at  $1666.5 \text{ cm}^{-1}$  was increased to  $A = 0.23$ . Photolysis with 290-1000-nm light from a high-pressure mercury arc for 30 min reduced the band to  $A = 0.22$ , and a 65-min exposure to 220-1000-nm light further reduced the  $1666.5\text{-cm}^{-1}$  absorption to  $0.21$  as determined from three sets of expanded scale scans.

Three experiments were done with a 90% carbon-13 enriched  $\text{CHF}_3$  sample. Trace (c) of Figure 2 shows the spectrum of an Ar/ $^{13}\text{CHF}_3 = 200/1$  sample deposited without argon resonance photolysis; note the weak water bands at  $1626$ ,  $1610$ , and  $1594 \text{ cm}^{-1}$  and the  $^{13}\text{CHF}_3$  combination band shifted to  $1619 \text{ cm}^{-1}$ . Trace (d) illustrates the spectrum of an Ar/ $^{13}\text{CHF}_3 = 800/1$  sample recorded after sample deposition with concurrent argon discharge photolysis for 17 h; note the sharp new band ( $2.0 \text{ cm}^{-1}$  full width at half-maximum) at  $1600.5 \text{ cm}^{-1}$  ( $A = 0.16$ ) and weak bands at  $1643.0$  ( $A = 0.035$ ) and  $1666.5 \text{ cm}^{-1}$  ( $A = 0.015$ ). Strong bands at  $1144$  and  $1137 \text{ cm}^{-1}$  and a weak absorption at  $1306 \text{ cm}^{-1}$  are probably due to the  $^{13}\text{CHF}_2$  radical. Sample warming to  $30\text{-}35 \text{ K}$  for 10 min reduced these bands markedly; the  $1600.5\text{-}$  and  $1643.0\text{-cm}^{-1}$  features decreased to  $A = 0.05$  and  $0.015$ , respectively. The  $^{13}\text{CF}_3$  absorption at  $1219 \text{ cm}^{-1}$  decreased slightly, and the  $^{13}\text{CF}_4$  band at  $1234 \text{ cm}^{-1}$  increased slightly. In an Ar/ $^{13}\text{CHF}_3 = 200/1$  photoionization study, the same bands were observed with increased intensities:  $1600.5$  ( $A = 0.20$ ),  $1643.0$  ( $0.040$ ), and  $1666.5 \text{ cm}^{-1}$  ( $0.02$ ) are of most interest here.

One experiment was done with an Ar/ $\text{CDF}_3 = 400/1$  sample. The strong, sharp  $1666.5\text{-cm}^{-1}$  ( $A = 0.28$ ) band was observed as in the  $\text{CHF}_3$  experiments along with  $\text{CF}_2$ ,  $\text{CF}_3$ , and  $\text{CF}_4$  and a strong  $645\text{-cm}^{-1}$  band ( $A = 0.33$ ).

## Discussion

The new product absorptions have been separated into four distinct groups by their behavior on high-pressure mercury arc photolysis, and their growth in sodium- $CF_3X$  samples upon medium-pressure mercury arc irradiation. These four groups—free radicals, daughter cations, parent cations, and parent anions—and the photophysical processes involved in these experiments will now be discussed.

**Free Radicals.** The  $CF_3$  and  $CF_2Cl$  free radicals have been observed by Milligan and Jacox in matrix photolysis studies,<sup>14,17</sup> and these neutral species are responsible for strong absorptions in the present studies. The  $CF_2Br$  free radical, found in  $CF_2Br_2$ <sup>18</sup> and  $CHF_2Br$ <sup>19</sup> photolysis experiments at 1197, 1137, and 685  $cm^{-1}$ , was also observed here. These free radicals were stable to mercury arc photolysis. In the  $CF_3I$  studies, new absorptions at 1126 and 627  $cm^{-1}$  are assigned here to the  $CF_2I$  free radical. Table IV contrasts the vibrational assignments to  $CF_2X$  free radicals. As is characteristic of iodo-carbon species, the  $CF_2I$  free radical absorptions were decreased by photolysis, as noted in Table III.

**Daughter Cations.** The new product absorptions in the 1320–1520- $cm^{-1}$  region and the 1666- $cm^{-1}$  band were linked by their stability to photolysis wavelengths longer than 340 nm and their gradual diminishment by 220–340-nm BH-6 light. The 1515- and 1415- $cm^{-1}$  absorptions have been assigned to the symmetric and antisymmetric C–F stretching modes of  $CF_2Cl^+$ ; the observation of  $^{13}CF_2Cl^+$  absorptions at 1473 and 1377  $cm^{-1}$  support this identification and assignment.<sup>8</sup> The 1484- and 1368- $cm^{-1}$  absorptions in the  $CF_3Br$  experiments, showing a slight displacement to lower frequency on bromine substitution, are appropriate for  $CF_2Br^+$ ; these absorptions have been observed in  $CHF_2Br$  and  $CF_2Br_2$  photoionization studies where the  $CF_2Br$  radical was also produced.<sup>18,19</sup> The 1433- and 1321- $cm^{-1}$  bands in  $CF_3I$  experiments show the same photolysis behavior and displacement to lower frequency on heavy halogen substitution, and they are assigned to the analogous modes of  $CF_2I^+$ . Weak bands at 1518 and 1400  $cm^{-1}$  in the  $CF_3Br$  experiments and at 1346  $cm^{-1}$  in the  $CF_3I$  studies were destroyed by 290–1000-nm photolysis; their mapping with the corresponding daughter cation absorptions suggests a  $CF_2X^+$  species perturbed by a nearby anion which photoneutralizes more readily than the isolated  $CF_2X^+$ . Table IV compares the  $CF_2X$  radical and cation vibrational data.

The only new product absorption above the  $CF_2X^+$  bands is the sharp feature at 1666.5  $cm^{-1}$  in all three  $CF_3X$  studies; this new band was not observed in  $CF_2Cl_2$  and  $CF_2Br_2$  investigations,<sup>8,18</sup> and it can be reasonably attributed to  $CF_3^+$ . Similar experiments with  $CHF_3$  and  $CDF_3$  produced this band at 1666.5  $cm^{-1}$  with increased intensity. Upon sample warming to allow diffusion of trapped species, the  $CF_3^+$  absorption decreased more than those of the  $CF_3$  radical, while  $CF_4$  absorptions increased.

Studies with 90%  $^{13}C$ -enriched  $CHF_3$  samples produced the  $^{13}C$  isotope at 1600.5  $cm^{-1}$  ( $A = 0.20$ ), with the expected intensity relative to the 1666.5- $cm^{-1}$  band ( $A = 0.020$ ) for a species containing a single carbon atom. The large  $^{13}C$  shift indicates a C–F stretching mode, but it is 20  $cm^{-1}$  larger than that calculated for the antisymmetric C–F stretching mode,  $\nu_3$ , of a trigonal planar  $CF_3^+$  species. This unexpectedly large carbon-13 shift can be explained by Fermi resonance<sup>20</sup> between  $(\nu_1 + \nu_4)$  and  $\nu_3$  for the  $^{13}CF_3^+$  species, since the new 1643.0- $cm^{-1}$  product band (Figure 2(d)) can be assigned to the combination  $(\nu_1 + \nu_4)$  mode. The calculated position of  $\nu_3$  of  $^{13}CF_3^+$ , 1621  $cm^{-1}$ , thus seems to coincide with the apparent position of  $(\nu_1 + \nu_4)$ , and these modes strongly interact and shift  $\nu_3$  down to 1600  $cm^{-1}$  and  $(\nu_1 + \nu_4)$  up to 1643  $cm^{-1}$ . Fermi resonance of this type is also found in  $CCl_4$ .<sup>9</sup> The  $(\nu_1 + \nu_4)$  combination band for  $^{12}CF_3^+$ , expected to lie 3–5 wave-

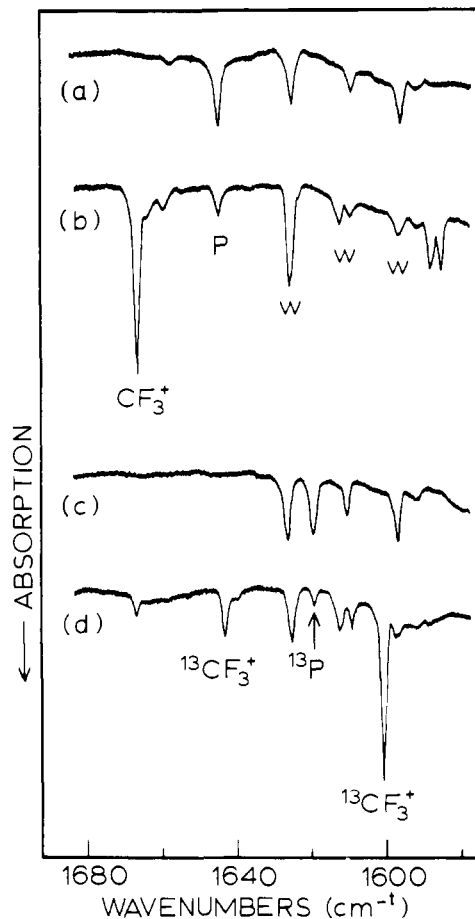


**Figure 2.** Infrared spectra in the 1580–1680- $cm^{-1}$  spectral region for fluoroform samples condensed with excess argon at 15 K. Spectrum (a) Ar/ $CHF_3$  = 200/1 with no discharge; trace (b) Ar/ $CHF_3$  = 800/1 with concurrent argon resonance photoionization. Spectrum (c) Ar/ $^{13}CHF_3$  = 200/1 with no discharge; trace (d) Ar/ $^{13}CHF_3$  = 800/1 with argon resonance photoionization. W denotes water absorptions.

**Table IV.** Comparison of Daughter Radical and Cation Vibrational Frequencies ( $cm^{-1}$ )<sup>a</sup>

Species	C–F symmetric	C–F antisymmetric	C–X symmetric
$CF_2I$	(1190)	1126	627
$CF_2I^+$	1433	1321	
$CF_2Br$	1197	1137	685
$CF_2Br^+$	1484	1368	
$CF_2Cl$	1208	1148	761
$CF_2Cl^+$	1515	1415	
$CF_3$	1084	1252	
$CF_3^+$	(1125)	1667	

<sup>a</sup> Parentheses denote estimated frequencies.

numbers above its  $^{13}C$  counterpart, is probably obscured by the 1626- $cm^{-1}$  water band, or it may be too weak to be observed here.

The combination  $(\nu_1 + \nu_4)$  for  $^{12}CF_3^+$  at approximately 1625  $cm^{-1}$  provides a basis for an estimate of the infrared inactive symmetric C–F bond stretching mode  $\nu_1$  of  $^{12}CF_3^+$  which might be observed in a high-resolution photoionization spectrum. The intensity of the  $\nu_2$  and  $\nu_4$  modes of  $BF_3$  are approximately a factor of 10 weaker than that of  $\nu_3$ , and the failure to observe these weaker fundamentals of  $CF_3^+$  in the present study is not surprising. However,  $\nu_4$  is estimated to be  $500 \pm 30$   $cm^{-1}$  since  $\nu_4 = 512$   $cm^{-1}$  for  $CF_3$ <sup>14</sup> and 480  $cm^{-1}$  for  $BF_3$ ,<sup>21</sup> which predicts  $\nu_1 = 1125 \pm 30$   $cm^{-1}$  for  $^{12}CF_3^+$ .

**Table V.** Comparison of Neutral Parent and Cation Vibrational Frequencies ( $\text{cm}^{-1}$ )

Species	$\nu_4$	$\nu_5$
	C-F antisymmetric stretching mode	F-C-F antisymmetric bending mode
$\text{CF}_3\text{Cl}$	1207	562
$\text{CF}_3\text{Cl}^+$	1299	455
$\text{CF}_3\text{Br}$	1202	550
$\text{CF}_3\text{Br}^+$	1293	469
	1255	
$\text{CF}_3\text{I}$	1176	543
$\text{CF}_3\text{I}^+$	1229	497

It is interesting to consider the bonding in  $\text{CF}_3^+$  in view of its substantially increased antisymmetric stretching frequency and the increased symmetric stretching frequency deduced from the  $\nu_1 + \nu_4$  band. This increase is considerable relative to the pyramidal  $\text{CF}_3$  species, as given in Table IV, and relative to the planar  $^{11}\text{BF}_3$  molecule ( $\nu_1 = 888$ ,  $\nu_3 = 1454 \text{ cm}^{-1}$ )<sup>21</sup> as well. From the well-known back-donation of fluorine 2p electron density to the positive carbon,<sup>4</sup> it is readily apparent that  $\text{CF}_3^+$  should exhibit extensive  $\pi$  (p-p) bonding, and the markedly increased  $\nu_3$  mode is consistent with this bonding model. The failure to prepare  $\text{CF}_3^+$  in superacid media<sup>7</sup> can be attributed to its great chemical reactivity with a fluoride ion donor rather than to physical instability.

**Parent Cations.** The major product band in each  $\text{CF}_3\text{X}$  experiment shifted from 1299 to 1293 or 1255  $\text{cm}^{-1}$  and to 1229  $\text{cm}^{-1}$  for  $\text{X} = \text{Cl}$ ,  $\text{Br}$ , and  $\text{I}$ . These bands were related by their common photodissociation with 340–1000-nm BH-6 light. The 1299- $\text{cm}^{-1}$  absorption has been assigned to the antisymmetric C-F stretching mode,  $\nu_4$ , of  $\text{CF}_3\text{Cl}^+$ ; the carbon-13 shift to 1262  $\text{cm}^{-1}$  confirms this assignment to  $\text{CF}_3\text{Cl}^+$ .<sup>8</sup> The correlation between  $\text{CF}_3\text{Cl}^+$  and  $\text{CF}_3\text{Cl}$ , and the trends for parent ion and neutral molecule upon bromine and iodine substitution for chlorine listed in Table V, support the 1293- and 1229- $\text{cm}^{-1}$  assignments to  $\text{CF}_3\text{Br}^+$  and  $\text{CF}_3\text{I}^+$ . It is presumed that the parent ion retains  $C_{3v}$  symmetry, although ionization removes an electron from one of the degenerate nonbonding p orbitals on the heavier halogen,<sup>22</sup> and the possibility of Jahn-Teller distortion in the antisymmetric C-F stretching mode<sup>23</sup> or matrix site asymmetry could lead to splitting in the degenerate  $\nu_4$  mode of  $\text{CF}_3\text{X}^+$ . In this regard, the 1299- $\text{cm}^{-1}$  absorption is reduced to a completely resolved 1302–1296- $\text{cm}^{-1}$  doublet with one-third of the original 1299- $\text{cm}^{-1}$  intensity upon 340–1000-nm photolysis. The most likely vibrational assignment for the 1293- and 1255- $\text{cm}^{-1}$  bands, which track together in many experiments, is to split components of the  $\nu_4$  mode of  $\text{CF}_3\text{Br}^+$ . A possible other component for the 1229- $\text{cm}^{-1}$   $\text{CF}_3\text{I}^+$  band was not found in the spectrum.

Additional absorptions labeled  $\text{P}^+$  at 734, 730, 455, and 416  $\text{cm}^{-1}$  in Figure 1(a) showed identical photolysis behavior with the 1299- $\text{cm}^{-1}$  band, and they are also assigned to  $\text{CF}_3\text{Cl}^+$ . The chlorine isotopic doublet at 734 and 730  $\text{cm}^{-1}$  identifies the C-Cl stretching mode,  $\nu_2$ , although the small  $^{13}\text{C}$  shift<sup>8</sup> for this absorption indicates a significant amount of symmetric C-F<sub>3</sub> deformation character for this mode. The 400- $\text{cm}^{-1}$  region in the spectra of Figure 1 shows another series of bands, 455, 469, and 497  $\text{cm}^{-1}$ , for the three  $\text{CF}_3\text{X}$  precursors, which exhibits a similar magnitude for the heavy halogen shift as the antisymmetric F-C-F bending mode,  $\nu_5$ , of the neutral parent. This evidence suggests a like assignment for the 455-, 469-, and 497- $\text{cm}^{-1}$  bands as given in Table V. The remaining weaker  $\text{CF}_3\text{Cl}^+$  absorption at 416  $\text{cm}^{-1}$  is probably due to the antisymmetric F-C-Cl deformation mode,  $\nu_6$ , since analogous modes were not observed for  $\text{CF}_3\text{Br}^+$  and  $\text{CF}_3\text{I}^+$ .

The weak band at 677  $\text{cm}^{-1}$  which follows the 1229- and

497- $\text{cm}^{-1}$   $\text{CF}_3\text{I}^+$  bands upon photolysis is probably due to the symmetric C-F<sub>3</sub> deformation mode of  $\text{CF}_3\text{I}^+$  which is slightly below the 744- $\text{cm}^{-1}$  value for the neutral molecule. No analogous band was found for  $\text{CF}_3\text{Br}^+$ .

The failure to observe the symmetric C-F<sub>3</sub> stretching mode for the  $\text{CF}_3\text{X}^+$  species is of some concern, since this mode,  $\nu_1$ , for the neutral molecule is almost as strong as the antisymmetric C-F<sub>3</sub> stretching mode. However, a similar separation between  $\nu_4$  and  $\nu_1$  of the  $\text{CF}_3\text{X}^+$  species would put  $\nu_1$  of  $\text{CF}_3\text{X}^+$  underneath the very strong  $\nu_4$  absorption of the  $\text{CF}_3\text{X}$  parent and prevent its detection in the present experiments. The observation of the two strong antisymmetric modes,  $\nu_4$  and  $\nu_5$ , of the parent cations and the photolysis behavior make a strong case for the infrared detection of the  $\text{CF}_3\text{X}^+$  species.

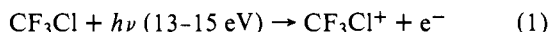
**Molecular Anions.** Absorptions observed near 900 and 660  $\text{cm}^{-1}$  in each  $\text{CF}_3\text{X}$  photoionization experiment were stable to 340–1000-nm BH-6 photolysis but were destroyed by 290–1000-nm light, which identifies a third new product species. Samples of each  $\text{CF}_3\text{X}$  compound and sodium were subjected to AH-4 photolysis, which has been demonstrated to provide photoelectrons for capture by molecules in the matrix,<sup>24</sup> and to form molecular anions by associative electron capture.<sup>1</sup> In the case of  $\text{CF}_3\text{Cl}$ , the 938- and 933- $\text{cm}^{-1}$  split band and a 666- $\text{cm}^{-1}$  feature appeared upon AH-4 photolysis, and likewise for  $\text{CF}_3\text{Br}$ , the 918- and 662- $\text{cm}^{-1}$  bands were produced. These same absorptions were also generated by argon resonance photoionization. In the  $\text{CF}_3\text{I}$ -sodium study photolysis produced a weak 892- $\text{cm}^{-1}$  absorption, but the 660- $\text{cm}^{-1}$  feature, observed in photoionization experiments, could not be detected on the side of the  $\text{CO}_2$  absorption. These observations indicate that a molecular anion has been formed.

The most likely explanation for the new molecular anion is associative electron capture by the parent. Since a heavy halogen dependence is indicated by the observed frequencies of 933, 918, and 893  $\text{cm}^{-1}$ , and fluoride elimination is energetically unfavorable, the new species is probably  $\text{CF}_3\text{X}^-$ . The extremely strong, similar absorptions at 849, 855, and 655  $\text{cm}^{-1}$  formed by the sodium- $\text{CF}_3\text{I}$  matrix reaction are probably due to the  $\text{CF}_3\text{I}^- \text{Na}^+$  charge-transfer complex, which was destroyed by 290–1000-nm mercury arc photolysis, as was the isolated radical anion.

The charge distribution in this molecular anion is of considerable interest. Several  $\text{CF}_3\text{X}^-$  radical anions have been observed in recent radiolysis studies where ESR spectra showed that the extra electron is located in an  $a_1$  ( $\sigma^*$ ) antibonding orbital composed of carbon and heavy halogen p orbitals.<sup>32</sup> On sample warming the  $\text{CF}_3\text{X}^-$  ESR signal was replaced by that of the  $\text{CF}_3$  radical. In addition, the  $\text{CF}_3\text{Cl}^-$  radical anion was prepared upon 320-nm photolysis by electron attachment reactions.<sup>32</sup> Since the latter photolytic production of  $\text{CF}_3\text{Cl}^-$  is comparable to the present sodium photoionization experiment where  $\text{CF}_3\text{Cl}^-$  was produced, it is concluded that the argon matrix-isolated  $\text{CF}_3\text{X}^-$  species is also a radical anion rather than a radical-halide ion complex. The  $\text{CF}_3\text{I}^-$  anion has recently been observed in gas-phase molecular beam studies where dissociation energy measurements indicate considerable stability for this anion.<sup>33</sup> The  $\text{CF}_3\text{X}^-$  radical anions have thus been produced in several types of experiments, indicating possible stabilization of the negative charge by the inductive effect of the fluorine atoms.

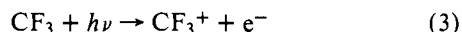
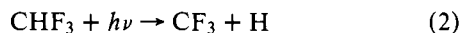
**Mechanism of Formation.** Evidence has been presented to support the resonance lamp function of the argon discharge tube.<sup>3,11,12</sup> It is proposed that the daughter and parent cations are formed from photoionization by argon resonance (1048 and 1067 Å, 11.62 and 11.83 eV) and higher energy radiation from the discharge<sup>12</sup> during condensation of the matrix sample. In the case of  $\text{CF}_3\text{Cl}^+$ , whose appearance potential is 12.45 eV from gas-phase photoionization studies,<sup>25</sup> the higher energy

radiation is required to photoionize CF<sub>3</sub>Cl:



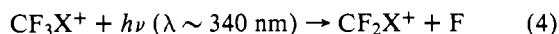
Even though the appearance potentials of CF<sub>3</sub>Br<sup>+</sup> and CF<sub>3</sub>I<sup>+</sup> are slightly less than that of CF<sub>3</sub>Cl<sup>+</sup>,<sup>22</sup> it is presumed that CF<sub>3</sub>Br<sup>+</sup> and CF<sub>3</sub>I<sup>+</sup> are also formed directly by higher energy argon emissions.<sup>12</sup>

The daughter cations CF<sub>3</sub><sup>+</sup> and CF<sub>2</sub>Cl<sup>+</sup> have even higher appearance potentials from CF<sub>3</sub>Cl.<sup>25</sup> These ions are most likely produced by photoionization of the radicals CF<sub>3</sub> and CF<sub>2</sub>Cl which are formed by photodissociation of the CF<sub>3</sub>Cl parent molecule. The CF<sub>2</sub>Br<sup>+</sup> and CF<sub>2</sub>I<sup>+</sup> species are probably made by secondary photoionization of the corresponding radicals as well. Since the appearance potential of CF<sub>3</sub><sup>+</sup> from CHF<sub>3</sub> is about 14 eV<sup>26</sup> it is probable that the CF<sub>3</sub><sup>+</sup> produced in fluoroform experiments also arises from photoionization of the radical, produced in very large yield in these experiments, which requires only 9.2 eV.<sup>27</sup>



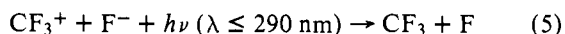
**Mechanism of Photolysis.** The photodestruction of parent cation absorptions by 290–1000-nm high-pressure mercury arc light which had a relatively minor effect on the daughter cation absorptions suggests a different photolysis mechanism for these two different types of cations. An examination of appearance potential data<sup>25</sup> reveals that approximately 2 eV is required to dissociate CF<sub>3</sub>Cl<sup>+</sup>, whereas 6 eV is required to eliminate fluorine from CF<sub>3</sub><sup>+</sup>. The dissociative transitions in each case will of course be at slightly higher energy, which places photolysis of CF<sub>3</sub>Cl<sup>+</sup> in the near ultraviolet, where the mercury arc is intense, and photodissociation of CF<sub>3</sub><sup>+</sup> in the vacuum ultraviolet, out of the mercury arc range.

It is proposed that the CF<sub>3</sub>X<sup>+</sup> species photodissociate with 340-nm light to eliminate fluorine which readily diffuses away through the matrix.<sup>28</sup>



A slight growth in the CF<sub>2</sub>X<sup>+</sup> absorptions in Tables I–III upon 340–1000-nm photodissociation of CF<sub>3</sub>X<sup>+</sup> confirms this mechanism. The fact that the CH<sub>3</sub>Cl<sup>+</sup> and CH<sub>3</sub>Br<sup>+</sup> ions have dissociative transition maxima near 320 nm in the gas phase, as determined from ICR and quadrupole mass spectrometer experiments,<sup>29,30</sup> further supports this argument for photodissociation of the CF<sub>3</sub>X<sup>+</sup> species.

The 1666-cm<sup>-1</sup> absorption of CF<sub>3</sub><sup>+</sup> was clearly diminished by irradiation with wavelengths between 340 and 290 nm, and after 2 h of exposure to high-intensity 220–1000-nm light, the 1666-cm<sup>-1</sup> band was reduced further. Since CF<sub>3</sub><sup>+</sup> cannot photodissociate with this radiation, it is suggested that photoneutralization takes place following photodetachment from electron traps in the matrix, most probably halide ions. The photodetachment thresholds for halide ions vary from 3.06 to 3.61 eV (approximately 400 to 340 nm)<sup>31</sup> and the cross sections can be expected to increase with increasing halide ion size. The observed photodestruction of CF<sub>3</sub><sup>+</sup> is consistent with a photoneutralization mechanism:



It is interesting to note that photoneutralization of CF<sub>3</sub><sup>+</sup> in CF<sub>3</sub>X experiments occurred most readily in the order I > Br > Cl > H (where F<sup>-</sup> probably served as the electron trap in the fluoroform experiments). The electron affinities of the halogens and the increasing cross sections for photodetachment from F<sup>-</sup>, Cl<sup>-</sup>, Br<sup>-</sup>, and I<sup>-</sup> nicely rationalize this trend.

In matrix photoionization experiments with CF<sub>3</sub>X compounds, fluorine molecules are probably produced and trapped.

Upon photolysis fluorine atoms are liberated for reaction with the matrix-isolated species. For example, the decrease in CF<sub>2</sub> absorption intensity and growth in CF<sub>3</sub> and CF<sub>4</sub> on photolysis (Table III) can be explained by fluorine atom reactions; even CF<sub>3</sub>I<sup>+</sup> absorptions increased on 500–1000-nm photolysis of the photoionized sample, which probably arose from the reaction of F atoms with CF<sub>2</sub>I<sup>+</sup>.

## Conclusions

The argon discharge photoionization of CF<sub>3</sub>Cl, CF<sub>3</sub>Br, and CF<sub>3</sub>I during condensation with excess argon at 15 K produced new infrared absorptions which were separated into groups by changes observed upon mercury arc photolysis. The absorptions most resistant to photolysis were assigned to the daughter cations CF<sub>3</sub><sup>+</sup> and CF<sub>2</sub>X<sup>+</sup>; their slow decrease upon high-intensity photolysis is attributed to photoneutralization by transfer of trapped electrons from halide ions. The assignment to CF<sub>3</sub><sup>+</sup> was confirmed by the observation of <sup>12</sup>CF<sub>3</sub><sup>+</sup> and <sup>13</sup>CF<sub>3</sub><sup>+</sup> from the <sup>12</sup>CHF<sub>3</sub> and <sup>13</sup>CHF<sub>3</sub> precursors.

The most photosensitive absorptions in these studies were assigned to the parent cations CF<sub>3</sub>X<sup>+</sup>, which photolyzed to eliminate fluorine and produce CF<sub>2</sub>X<sup>+</sup>. Several bands with intermediate photolysis behavior were also produced in photolysis experiments with sodium which indicates their assignment to molecular anions; the most likely explanation for these bands is the parent radical anion CF<sub>3</sub>X<sup>-</sup>.

The matrix photoionization technique has provided infrared spectroscopic data on a number of ions heretofore observed only in gas-phase mass spectra. Of most interest is the observation of CF<sub>3</sub><sup>+</sup> and its very high ν<sub>3</sub> fundamental which is consistent with extensive π(p-p) bonding in this molecular cation.

**Acknowledgment** is made to the donors of the Petroleum Research Fund, administered by the American Chemical Society, for support of this research.

## References and Notes

- (1) M. E. Jacox and D. E. Milligan, *J. Chem. Phys.*, **54**, 3935 (1971).
- (2) L. Andrews, J. M. Grzybowski, and R. O. Allen, *J. Phys. Chem.*, **79**, 904 (1975).
- (3) F. T. Prochaska and L. Andrews, *J. Chem. Phys.*, **67**, 1091 (1977).
- (4) G. A. Olah and M. B. Comisarow, *J. Am. Chem. Soc.*, **91**, 2955 (1969).
- (5) G. A. Olah, Y. Halpern, and Y. K. Mo, *J. Am. Chem. Soc.*, **94**, 3551 (1972).
- (6) G. A. Olah and Y. K. Mo, *J. Org. Chem.*, **37**, 1029 (1972).
- (7) G. A. Olah and Y. K. Mo in "Carbonium Ions", Vol. V, Wiley-Interscience, New York, N.Y., 1976.
- (8) F. T. Prochaska and L. Andrews, *J. Chem. Phys.*, to be published.
- (9) L. Andrews, *J. Phys. Chem.*, **71**, 2761 (1967); *J. Chem. Phys.*, **48**, 972 (1968).
- (10) L. Andrews, *J. Chem. Phys.*, **54**, 4935 (1971).
- (11) C. A. Wight, B. S. Ault, and L. Andrews, *J. Chem. Phys.*, **65**, 1244 (1976).
- (12) L. Andrews, D. E. Tevault, and R. R. Smardzewski, *Appl. Spectrosc.*, **32**, in press.
- (13) R. L. Reddington and D. E. Milligan, *J. Chem. Phys.*, **39**, 1276 (1963).
- (14) D. E. Milligan and M. E. Jacox, *J. Chem. Phys.*, **48**, 2265 (1968).
- (15) E. K. Plyer and W. S. Benedict, *J. Res. Natl. Bur. Stand.*, **47**, 202 (1951).
- (16) T. G. Carver and L. Andrews, *J. Chem. Phys.*, **50**, 5100 (1969).
- (17) D. E. Milligan, M. E. Jacox, J. H. McAuley, and C. E. Smith, *J. Mol. Spectrosc.*, **45**, 377 (1973).
- (18) F. T. Prochaska and L. Andrews, to be published.
- (19) C. A. Wight and L. Andrews, unpublished results.
- (20) G. Herzberg, "Infrared and Raman Spectra", Van Nostrand, Princeton, N.J., 1945, p 310.
- (21) K. Nakamoto, "Infrared Spectra of Inorganic and Coordination Compounds", Wiley, New York, N.Y., 1963.
- (22) J. Doucet, P. Sauvageau, and C. Sandorty, *J. Chem. Phys.*, **58**, 3708 (1973).
- (23) G. Herzberg, "Electronic Spectra of Polyatomic Molecules", Van Nostrand, Princeton, N.J., 1966, p 40.
- (24) P. H. Kasal, *Acc. Chem. Res.*, **4**, 329 (1971).

- (25) H. W. Jochims, W. Lohr, and H. Baumgartel, *Ber. Bunsenges. Phys. Chem.*, **80**, 130 (1976).  
 (26) C. R. Brundle, M. B. Robin, and H. Basch, *J. Chem. Phys.*, **53**, 2196 (1970).  
 (27) T. A. Walter, C. Lifshitz, W. A. Chupka, and J. Berkowitz, *J. Chem. Phys.*, **51**, 3531 (1969).  
 (28) L. Andrews, *J. Chem. Phys.*, **57**, 51 (1972).  
 (29) R. C. Dunbar, *J. Am. Chem. Soc.*, **93**, 4345 (1971).  
 (30) M. L. Vestal and J. H. Futrell, *Chem. Phys. Lett.*, **28**, 559 (1974).  
 (31) R. S. Berry and C. W. Reimann, *J. Chem. Phys.*, **38**, 1540 (1963).  
 (32) A. Hasegawa and F. Williams, *Chem. Phys. Lett.*, **46**, 66 (1977).  
 (33) P. E. McNamee, K. Lacmann, and D. R. Herschbach, *Faraday Discuss. Chem. Soc.*, **55**, 318 (1973); S. Y. Tang, B. P. Mathur, E. W. Rothe, and G. P. Reck, *J. Chem. Phys.*, **64**, 1270 (1976).

## Electron Spin Resonance Studies of the Reaction of Lithium Atoms with Lewis Bases in Argon Matrices: Formation of Reactive Intermediates. 1. Water and Ammonia<sup>†</sup>

Paul F. Meier, Robert H. Hauge, and John L. Margrave\*

Contribution from the Department of Chemistry, Rice University, Houston, Texas 77001. Received June 27, 1977

**Abstract:** The reactions of lithium atoms with water and with ammonia have been studied at liquid helium temperatures using ESR matrix isolation spectroscopy techniques. These experiments indicate the formation of molecular complexes in both reactions, with the stability of the complexes being due to the sharing of the Lewis base lone pair electrons with lithium. The complexes involve the interaction of a lithium atom with a single molecule in the case of NH<sub>3</sub> and H<sub>2</sub>O; in addition, the lithium-water reaction yields a complex involving two H<sub>2</sub>O molecules. Electronic *g* values and hyperfine interaction constants are reported for the complexes. The matrix isolated complexes were photolyzed by near-visible light. Possible reaction products of this photolysis are discussed for each complex.

### Introduction

The alkali metal atoms, because of their electronic structures, constitute a group of very reactive elements. Reactions with molecules such as water and ammonia (classic Lewis bases) are spontaneous or easily initiated reactions at room temperature. Comparable chemical reactivity, however, is not expected on a monomolecular scale at cryogenic temperatures, as reaction rates are greatly impeded by reduced thermal activity.

Matrix isolation ESR has been used before to characterize small atomic and molecular radicals.<sup>1,2</sup> By this method, the molecular species to be observed are isolated at high dilution in an unreactive matrix which restricts thermal mobility and allows the preservation of unstable reactive intermediates and radical molecules. Free radicals may be generated in the gaseous state and then deposited in some matrix material; alternatively, radical species may be generated in situ in the matrix. The hyperfine structure observed in ESR spectra frequently allows complete identification of small systems. Recent work<sup>3,4</sup> has shown that matrix isolation is suitable for producing and studying reaction intermediates. The long-range goal of this approach is to study the chemical and physical properties of isolated chemical systems and apply these results to large-scale reactive systems.

In this work, lithium was reacted with water and ammonia on a molecular scale via codeposition with excess argon at approximately 15 K. Since Li(<sup>2</sup>S) is paramagnetic in the atomic state, electron spin resonance (ESR) spectroscopy was used to investigate the extent of reaction of lithium with water and ammonia. Because ESR directly measures spin density, the experimental results provide a quantitative measure of the change in spin density at the lithium nucleus resulting from the formation of Li<sub>n</sub>(H<sub>2</sub>O)<sub>m</sub> and Li<sub>n</sub>(NH<sub>3</sub>)<sub>m</sub> complexes observed in these experiments. This change in spin density at

the lithium nucleus can be caused by an electron transfer mechanism and concomitant atomic rehybridization. If these complexes may be induced to react further and form the same reaction products as those observed under standard conditions (STP), it is plausible that these species are a good representation of the intermediate species leading to the products observed under standard conditions.

### Theory

Fundamental to the analysis of the data for a paramagnetic system is the construction of a spin Hamiltonian for the system and the subsequent eigenvalue solution. In systems possessing spherical symmetry, such as lithium, the spin Hamiltonian is<sup>5</sup>

$$\mathcal{H} = g\beta\mathbf{H}\cdot\mathbf{S} + A\mathbf{S}\cdot\mathbf{I} - g_n\beta_n\mathbf{H}\cdot\mathbf{I} \quad (1)$$

*g* and *g<sub>n</sub>* represent the electronic and nuclear *g* factors while  $\beta$  and  $\beta_n$  represent the Bohr and nuclear magneton, respectively. **S** and **I** are the spin and nuclear moments, and **H** represents the applied magnetic field. The first and third terms correspond to the Zeeman energies in a magnetic field and the second term is the hyperfine Fermi-contact interaction energy. *A* is the hyperfine coupling constant, and is related to the unpaired spin density ( $|\psi(0)|^2$ ) at the nucleus.

$$A = (8\pi/3)g\beta g_n\beta_n|\psi(0)|^2 \quad (2)$$

For a spherical system, the electronic *g* tensor and the hyperfine coupling constant are isotropic and diagonal.

When *S* = 1/2, the equation  $\mathcal{H}\psi_n = E\psi_n$  may be solved in closed form; the solution to the eigenvalue problem is well known and is called the Breit-Rabi formula.<sup>6</sup>

When lithium forms a complex with water or ammonia, the spherical symmetry of atomic lithium is destroyed. Proper analysis of the new system would require making a judgement on the new symmetry of this complex; then a new spin Hamiltonian can be formulated and the subsequent eigenvalue problem solved. Even if a symmetry could be assigned to the

<sup>†</sup> Presented in part at the First Chemical Congress of the North American Continent, Mexico City, Mexico, Nov 30-Dec 5, 1975, and at the Conference on Magnetohydrodynamics, Argonne National Laboratories, Chicago, Ill., April 1977.